ACS OMEGA

Open Access

http://pubs.acs.org/journal/acsodf

Article

Lysine-Polydopamine Nanocrystals Loaded with the Codrug Abemaciclib-Flurbiprofen for Oral Treatment of Cancer

Ting Sun, Faxing Zhang, Yuyi Xu, Xiaowei Wang, Jiajia Jia, Lihong Sang, Ji Li,* Dongkai Wang,* and Zhiguo Yu*

Cite This: *ACS Omega* 2024, 9, 18137−18147

Read Online

ACCESS | Metrics & More | Article Recommendations | Supporting Information

ABSTRACT: Nonsteroidal anti-inflammatory drugs (NSAIDs) combined with chemotherapeutic agents for the treatment of colorectal cancer (CRC) are a promising therapeutic strategy. NSAIDs can effectively boost the antitumor efficacy of chemotherapeutic agents by inhibiting the synthesis of COX-2. However, hazardous side effects and barriers to oral drug absorption are the main challenges for combination therapy with chemotherapeutics and NSAIDs. To address these issues, a safe and effective lysine−polydopamine@abemaciclib-flurbiprofen (Flu) codrug nanocrystal (Lys-PDA@AF NCs) was designed. Abemaciclib (Abe), a novel and effective inhibitor of the CDK4/6 enzyme, and Flu were joined to prepare Abemaciclib-Flu codrug (AF) by amide bonds, and then the AF was made into nanocrystals. Lysine-modified polydopamine was selected as a shell to encapsulate nanocrystals to enhance intestinal adhesion and penetration and lengthen the duration time of drugs *in vivo*. Nuclear magnetic resonance, Fourier transform infrared, Massspectrometry, X-ray photoelectron spectroscopy, Transmission electron microscopy, and drug loading were used to evaluate the physicochemical characteristics of the nanocrystals. In our study, Abe and Flu were released to exert their synergistic effect when the amide bond of AF was broken and the amide bond was sensitive to cathepsin B which is overexpressed in most tumor tissues, thus increasing the selectivity of the drug to the tumor. The results showed that Lys-PDA@AF NCs had higher cytotoxicity for CRC cell with an IC_{50} of 4.86 μg/mL. Additionally, pharmacokinetics showed that Abe and Flu had similar absorption rates in the Lys-PDA@AF NCs group, improving the safety of combination therapy. Meanwhile, *in vivo* experiments showed that Lys-PDA@AF NCs had excellent antitumor effects and safety. Overall, it was anticipated that the created Lys-PDA@AF NCs would be a potential method for treating cancer.

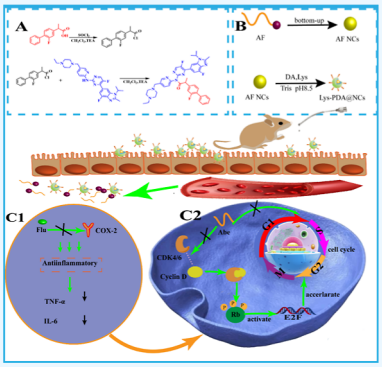

1. INTRODUCTION

Abemaciclib (Abe) is a novel and effective inhibitor of the CDK4/6 enzyme. Abe inhibits the E2F pathway to prevent cells from transitioning from G1 to S by binding to CDK4/6 enzymes, exhibiting stable efficacy in a variety of advanced solid tumors, including colorectal cancer (CRC).[1−3] The very fatal malignancy CRC demonstrates COX-2 overexpression and is closely linked to chronic inflammation.[4−8] COX-2 can accelerate the growth of tumors by increasing the level of the proangiogenic protein BAX. Additionally, the likelihood of tumor invasion and metastasis is also increased due to the correlation between epithelial-to-mesenchymal transition and COX-2.[9,10] Therefore, the combination of nonsteroidal anti-inflammatory drugs (NSAIDs) with chemotherapeutic agents is a promising therapeutic strategy for the treatment of CRC. However, combination therapy still has many challenges: poor oral absorption due to the complex gastrointestinal environment and toxic side effects resulting from multiple causes.[11−15]

Based on this, codrugs are a promising method for solving the drawbacks and exploiting the advantages of combination therapy. As an NSAID, flurbiprofen (Flu) possesses a carboxyl group that can join chemotherapeutic agents via amide or ester bonds to generate a codrug that can suppress COX-2 and inflammatory factors, hence boosting the antitumor effectiveness of chemotherapeutic agents. The formation of codrugs by amide bonds has selectivity toward tumor sites because amide bonds are sensitive to cathepsin B, which is overexpressed in the majority of CRC tissues. In addition, the codrug may have a better affinity for the receptor, so it may not only work by releasing the original drug, but as a new entity itself, may also have some antitumor efficacy, making the codrug more therapeutically effective.[16,17] The fact that Abe and Flu, released *in vivo* by codrugs, have similar absorption rates, which could improve the safety and efficacy of the combination therapy, is of greater interest.[18−20]

Subsequently, the codrug was converted into nanocrystals in the hope of increasing the oral absorption by changing the size,

Received: December 19, 2023
Revised: March 29, 2024
Accepted: April 2, 2024
Published: April 11, 2024

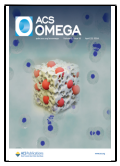

shape, and surface properties of the nanocrystals. Then, polydopamine (PDA) was selected to encapsulate nanocrystals to improve the mucus adhesion and mucus penetration of nanocrystals.[21,22] PDA has a structure similar to that of the mussel adhesion protein. PDA can be coated on a wide range of materials and particles due to its strong property of adhesion.[23,24] Additionally, PDA also has the ability of mucus to penetrate due to its amphiphilic nature.[25] Surface modification with alkaline amino acids allows the modified PDA to be nearly electrically neutral and, thus, more likely to cross the mucus barrier. Therefore, PDA is a promising drug carrier material.[26,27]

In this study, a codrug made from Abe and Flu was presented, and Lys-PDA@AF NCs were successfully prepared by encasing nanocrystals in PDA modified with lysine. The results supported the use of Abe and Flu in combination therapy because of their synergistic effects. The oral absorption, anticancer effectiveness, and safety of combination therapy were all improved with Lys-PDA@AF NCs. A large number of studies were carried out to support this notion.

2. MATERIALS AND METHODS

2.1. Materials. All drugs and reagents were of chromatographic grade, used directly, and not purified.

Abe (98%), Flu (98%), ketoprofen (99%), dopamine hydrochloride, L-lysine, and palbociclib (99%) were purchased from Aladdin Reagent Co., Ltd. (Shanghai). Cathepsin B and mucin were purchased from Sigma-Aldrich. Pepsin and trypsin were purchased from Dalian Meilun Biotechnology Co., Ltd. Cell experiment-related reagents (trypsin, RPMI-1640 culture medium, PBS, MTT) were obtained from Dalian Meilun Biotechnology Co., Ltd. CT-26 cells were obtained from Shenyang Pharmaceutical University, BAL B/C mice and Sprague−Dawley rats were provided by the animal experiment center of Shenyang Pharmaceutical University, and the animal research met the ethical requirements.

2.2. Synthesis of Codrug AF. 500 mg of Flu (500 mg) was dissolved in 8 mL of dichloromethane (CH_2Cl_2). Then, 200 μL of sulfoxide chloride ($SOCl_2$) and 150 μL of triethylamine were added dropwise with stirring, and the mixture was reacted at 35 °C for 5 h.

Abe (1 g) was dissolved in 8 mL of CH_2Cl_2, and then the Abe solution was slowly added to the above solution. Triethylamine (150 μL) was added dropwise and reacted for 18 h. When the reaction was over, the reaction solution was evaporated, an appropriate amount of water was added to dissolve the dry powder, and then 1 mol/L sodium hydroxide solution was added dropwise until no precipitation occurred. The precipitate was collected by filtration and refined by column chromatography to give the yellow product. The yield was 89%. Structural analysis of AF was done by 1H nuclear magnetic resonance (NMR), IR, and mass spectrometry (MS).

2.3. Stability Studies. *2.3.1. Chemical Stability.* The stability of AF was investigated. In summary, 100 μg/mL AF was prepared in buffers of pH 1.2 [0.2% sodium dodecyl sulfate (SDS)], pH 5.0 (0.2% SDS), and pH 6.8 (0.2% SDS). Subsequently, each solution was incubated at 37 °C for 24 h. The incubated solution was removed at a specific time. Each point of the solution was determined by high-performance liquid chromatography (HPLC, Shimadzu, Japan). Chromatographic conditions (method 1) are shown in the Supporting Information.

2.3.2. Simulated Gastrointestinal Stability. AF solutions (100 μg/mL) were prepared with artificial gastric and artificial intestinal fluids, incubated at 37 °C for 12 h, and removed at a specific time. Each point of the solution was determined by HPLC. Chromatographic conditions (method 1) are shown in the Supporting Information.

2.3.3. Enzymatic Stability. The stability of AF in the presence of cathepsin B (3 U/mL) was investigated. AF (100 μg/mL) was incubated at 37 °C in buffers at pH 5.0 (0.2% SDS and 3 U/mL cathepsin B) for 12 h, and the incubated solution was removed at a specific time. The results were compared to the chemical stability in pH 5.0 (0.2% SDS) buffer. Each point of the solution was determined by HPLC. Chromatographic conditions (method 1) are shown in the Supporting Information.

2.4. Molecular Docking Prediction. To analyze whether AF as a new entity has the ability to bind to CDK4/6 enzymes, the affinity of AF to the CDK4/6 enzyme was predicted using Autodock Vina and Discovery Studio 2016 software. The protein numbers of CDK4 and CDK6 used for molecular docking were 2w96 and 5L2T, respectively. First, the protein molecules and ligand molecules were subjected to water removal and hydrogenation. Subsequently, a docking box was set up, and molecular docking was performed using Autodock vina to calculate the affinity energy. Finally, Discovery Studio was used to analyze the interaction between AF and CDK4/6.

2.5. Preparation of Lys-PDA@AF NCs. 50 mg portion of AF was dissolved in 1 mL of methanol. The solution was quickly added to a Tris solution containing 0.1% sodium deoxycholate at pH 8.5, stirred for 1 min, and sonicated for 10 min to obtain an emulsion of nanocrystals. Then, 60 mg of dopamine hydrochloride (2 mg/mL) and 60 mg of lysine were added to the nanocrystals and stirred at room temperature for 4 h. The nanocrystals were centrifuged at 12,000 rpm for 15 min, and the supernatant was removed to obtain the Lys-PDA@AF NCs.

2.6. Characterization of Lys-PDA@AF NCs. The Lys-PDA@AF NCs were characterized by X-ray photoelectron spectroscopy (XPS) (Thermo Kalpha, USA) and Fourier transform infrared (FTIR) (Thermo Scientific Nicolet iS5, USA). The particle size and zeta potential were determined with a Malvern PANalytical analyzer (Nano-ZS 90, Malvern, UK). Meanwhile, the morphology of the Lys-PDA@AF NCs was observed by using transmission electron microscopy (TEM) (JEOL JEM 2100F, Japan). The drug loading was determined as follows: Lys-PDA@AF NCs were dissolved by adding methanol. After shaking for 2 min, the solution was centrifuged at 12,000 rpm for 5 min, the supernatant was collected, and the drug loading was determined by HPLC. The drug loading was calculated by eq 1.

$$\text{Drug loading (\%)} = \frac{W_{\text{AF}}}{W_{\text{formulation}}} \times 100\% \quad (1)$$

(W_{AF} and $W_{\text{formulation}}$ were defined as the weights of AF and formulation).

2.7. Drug Release in Vitro. *in vitro* was determined by means of the dialysis method. Briefly, the Abe, AF, and Lys-PDA@AF NCs were placed in different dialysis bags (MW = 3000 Da), and the bags were placed in release media (pH 1.2 and pH 6.8, with 0.2% SDS, 100 mL). Two mL portion of the solution was removed at specific times, and an equal volume of fresh medium was added. The cumulative release was

https://doi.org/10.1021/acsomega.3c10142
ACS Omega 2024, 9, 18137−18147

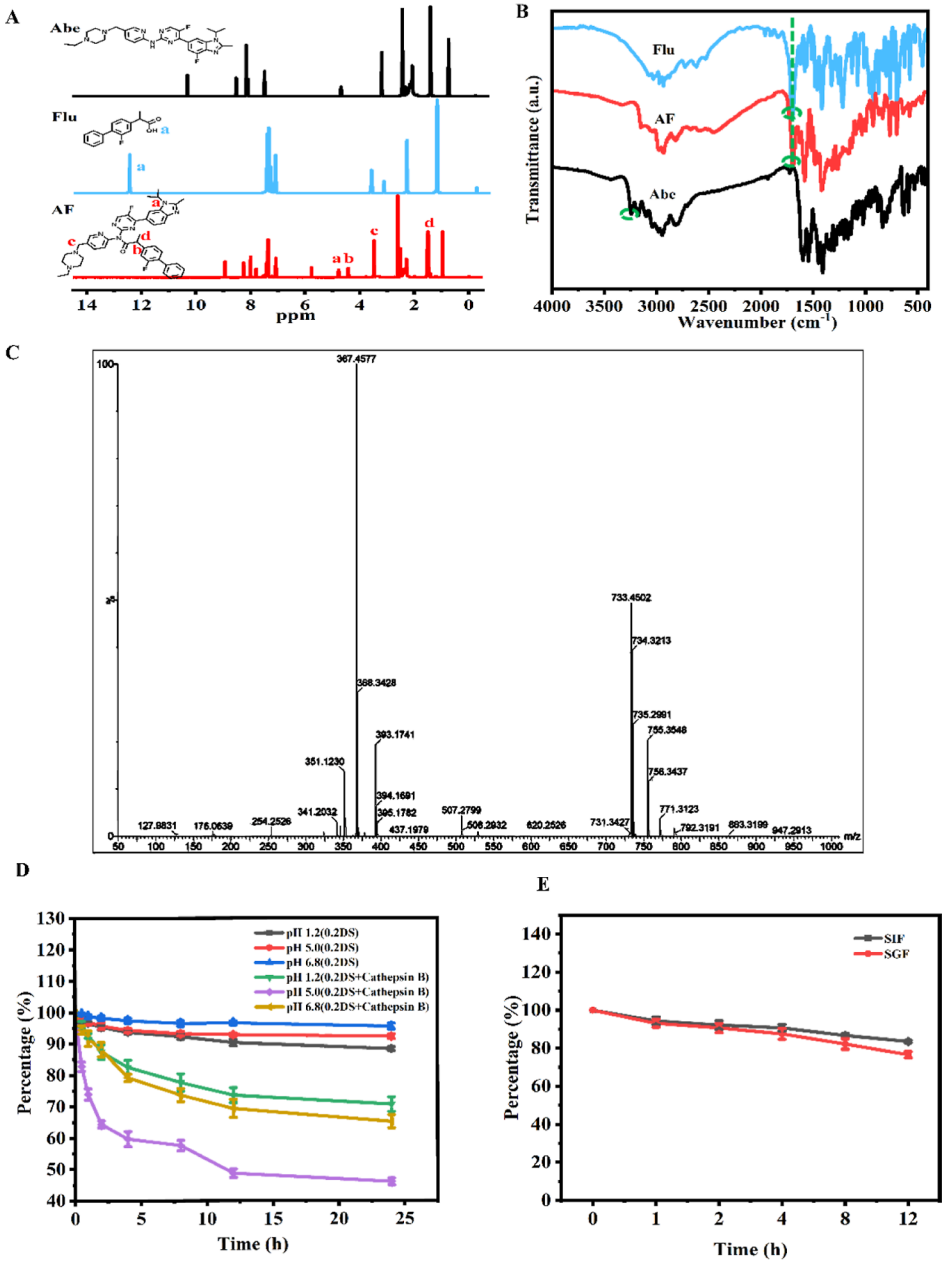

Figure 1. (A) NMR hydrogen spectra of Abe, Flu, and AF. (B) FTIR spectra of Abe, Flu, and AF. (C) Mass spectrum of AF. (D) Stability of AF with or without cathepsin B in different buffers. (E) Stability of AF in artificial gastric and intestinal fluids. Data are exhibited as mean ± SD (n = 3).

measured by HPLC. Chromatographic conditions (method 1) are provided in the Supporting Information.

2.8. In Vitro Cytotoxicity. The cytotoxicity of AF on CT26 cells was measured by the MTT method. Abe and Flu were used as positive controls. CT26 cells at the logarithmic growth stage were inoculated on 96-well plates at 1×10^4/well at 37 °C for 12 h. After removing the culture medium, different concentrations (0, 5, 10, 20, 40, and 80 μg/mL) of control solutions, physical mixture (Abe + Flu) solution, and Lys-PDA@AF NC solutions were added. After 48 h, 20 μL (5 mg/mL) of the MTT indicator was added and incubated for 4 h. Adding 150 L of dimethyl sulfoxide and shaking for 5 min were the final step. The IC_{50} value was calculated by measuring the absorbance at 570 nm using a microplate reader. Concentrations in each group were converted to Abe for the calculations.

The combination index (CI) of Abe and Flu was calculated by the cell viability. The formula was calculated as CI % = (D)A/(d)A + (D)B/(d)B, where (D)A and (D)B were the individual doses of drugs A and B needed to kill 50% of the tumor cells in the combination treatment, respectively. (d)A and (d)B are the IC_{50} values for drug A and drug B, respectively (additive CI = 1, synergistic CI < 1, and or antagonistic CI > 1).

2.9. Intestinal Absorption. *2.9.1. In Situ Perfusion.* Evaluation of the intestinal permeability of Lys-PDA@AF NCs was performed using an in situ intestinal perfusion test in rats. The abdominal cavity (approximately 3 cm long) was opened along the midline of the abdomen; a small incision was made in the upper duodenum and lower ileum, and a glass tube (0.5 cm) was inserted in each. The rats were connected in series into a circulation device. The tube was circulated at 5 mL/min

https://doi.org/10.1021/acsomega.3c10142
ACS Omega 2024, 9, 18137−18147

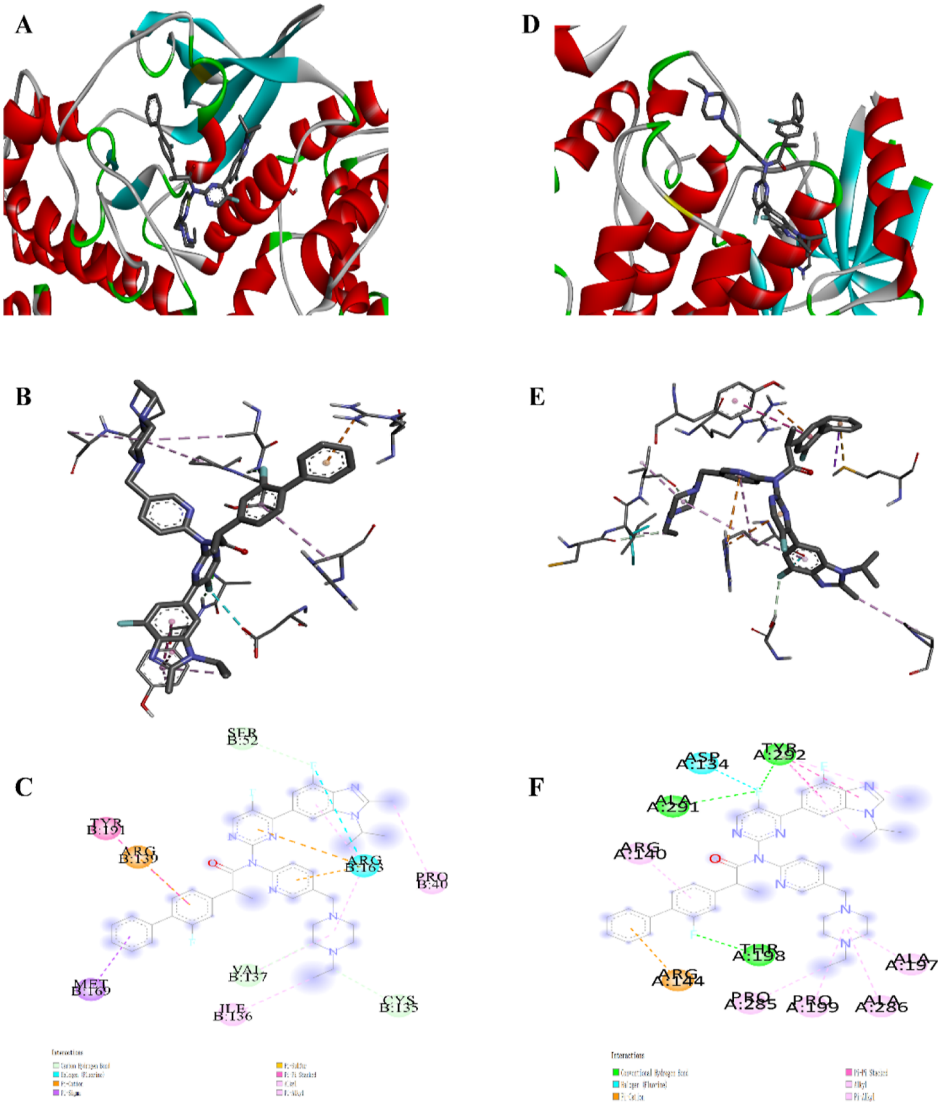

Figure 2. (A−C) Visualization of the molecular docking of AF and 2w9b protein. (s*D-E-F*) The visualization of the molecular docking of AF and 5L2T protein.

for 10 min and then adjusted to 2.5 mL/min and samples were taken every 15 min while replenishing the phenol red solution and collected for 90 min. The absorption rate constant Ka was found by linearizing the logarithm of the remaining drug amount against time and calculating the hourly absorption rate according to eq 2.

$$\text{hourly absorption rate } (\%) = \frac{m_0 - m_{90}}{m_0} \times 100\% \quad (2)$$

(m_0 and m_{90} were defined as the remaining dose of zero time and the remaining dose of 90 min).

2.9.2. Mucin-Binding Assay. Lys-PDA@AF NCs and AF solutions were prepared using mucin solution as the solvent. A sample of 100 μL of each solution was taken at different times (1, 2, 4, and 8 h) and then centrifuged at 4000 rpm for 15 min, and the supernatant was extracted to be measured.

2.10. Pharmacokinetic and Tissue Distribution Study. Eighteen SD rats were randomly divided into two groups. They were fed 12 h prior to the test but had free access to water. Rats in each group were given a physical mixture (Abe + Flu) and Lys-PDA @AF NCs by gavage. The doses administered were equivalent to 31.5 mg/kg Abe and 15.2 mg/kg Flu, and the $t_{1/2}$ and AUC of different groups were compared. The blood concentration of each group was determined by HPLC-MS/MS. Chromatographic conditions and mass spectrometric conditions (method 2) are provided in the Supporting Information.

To assess the tissue distribution of drugs, the rats in different groups were orally administered a physical mixture (Abe + Flu) and Lys-PDA@AF NCs, (equivalent to 31.5 mg/kg Abe and 15.2 mg/kg Flu) and then sacrificed at regular intervals. Afterward, the heart, liver, spleen, lung, kidney, stomach, and intestine of the rats were removed. The concentrations of Abe, Flu, and AF in the tissues were determined by HPLC. Chromatographic conditions (method 3) are provided in the Supporting Information.

2.11. *In Vivo* Antitumor Activity. The CT26 cell suspension was injected subcutaneously into six-week-old BAL B/C mice. When the tumors grew to 100 mm^3, the rats were divided into four groups, and then saline, Abe, physical mixture (Abe + Flu), and Lys-PDA@AF NCs (equivalent to 52 mg/kg Abe and 25 mg/kg Flu) were administered by gavage for 14 days to evaluate the growth of tumors. The

https://doi.org/10.1021/acsomega.3c10142
ACS Omega 2024, 9, 18137−18147

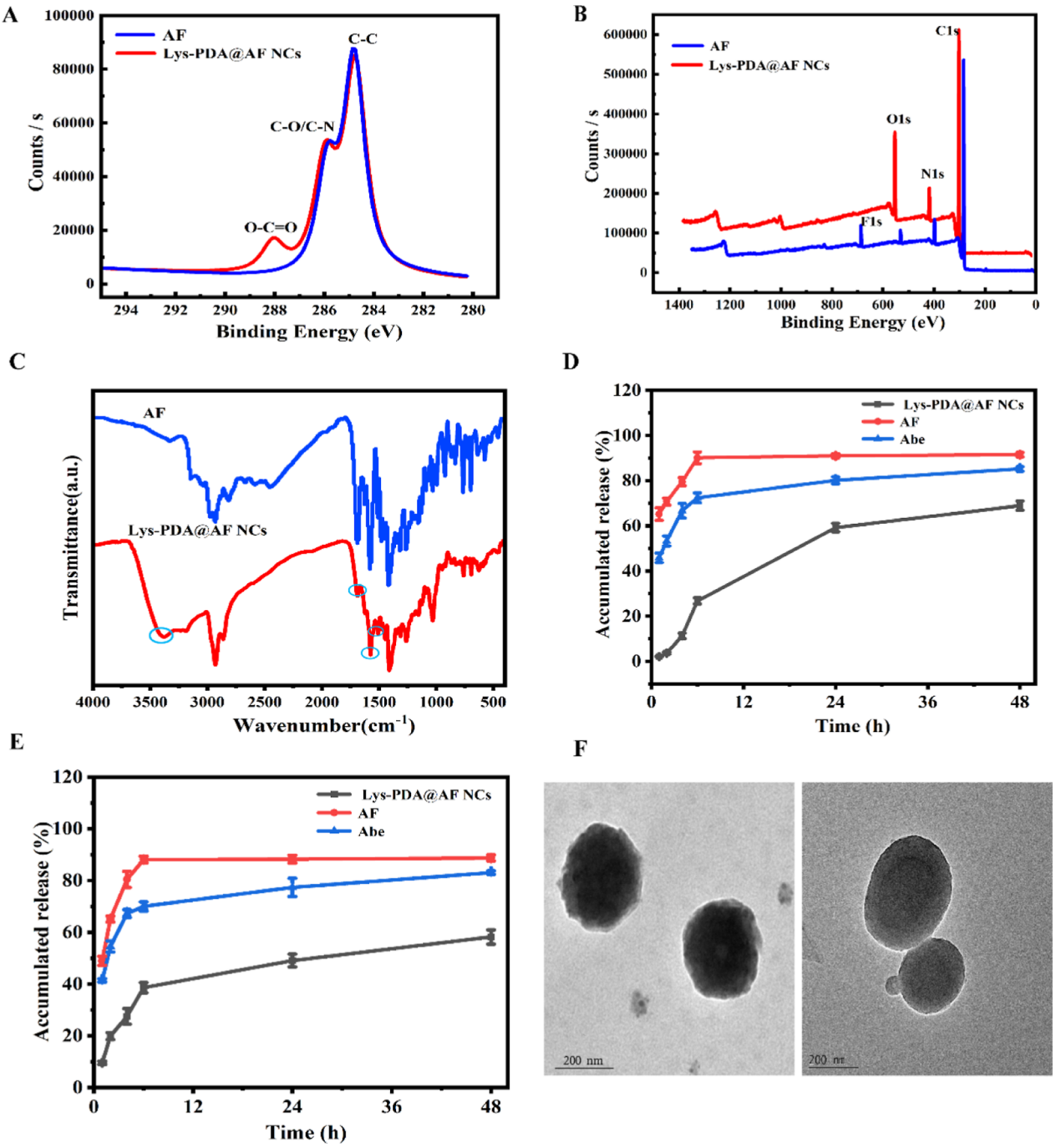

Figure 3. Characterization of Lys-PDA@AF NCs. (A,B) XPS of AF and Lys-PDA@AF NCs. (C) The FTIR spectra of Lys-PDA@AF NCs. The release behavior of AF and Lys-PDA@AF NCs in different media. (D) pH 1.2 and (E) pH 6.8. (F) TEM of Lys-PDA@AF NCs. Data are exhibited as mean ± SD (n = 3).

change in tumor volume was calculated using eq 3. Meanwhile, apoptosis, necrosis, and proliferation of tumors were evaluated by TUNEL, HE, and ki67 staining at the end of the test. Meanwhile, IL-6 and TNF-α levels in tumor tissues were measured by enzyme-linked immune sorbent assay (ELISA) to evaluate inflammatory factors.

$$\text{Tumour volume } (\%) = \frac{a \times b^2}{2} \tag{3}$$

(a is the long diameter of the tumor and b is the short diameter of the tumor).

2.12. Safety Evaluation. To evaluate the safety of the formulation, whole blood analysis was performed to evaluate the number of neutropenia, platelets, leukocytes, and erythrocytes. Aspartate aminotransferase (AST), alanine aminotransferase (ALT), urea nitrogen (BUN), and creatinine (CR) were measured to evaluate whether the Lys-PDA@AF NCs were hepatorenal toxic. HE staining analysis of the major organs (heart, liver, spleen, lung, and kidney) was performed to evaluate whether there was damage to normal tissues.

https://doi.org/10.1021/acsomega.3c10142
ACS Omega 2024, 9, 18137−18147

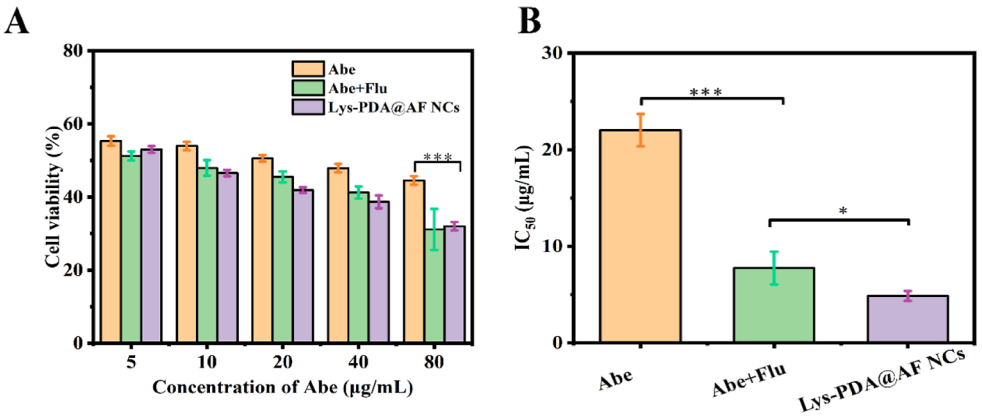

Figure 4. (A) Cell viability of different groups. (B) The IC_{50} values of different groups. Data are exhibited as mean ± SD (n = 5).*P < 0.05, **P < 0.01, and ***P < 0.001.

3. RESULTS AND DISCUSSION

3.1. Synthesis of AF Codrug. The synthesis route is shown in Figure S1 (Supporting Information). The conversion of the carboxylic acid group in Flu to acyl chloride was able to increase the reaction activity. The ^{1}H NMR spectrum of AF showed that δ4.78 (s, 1H) was attributed to the proton on the tertiary carbon of the isopropyl of Abe, δ3.56 (q, 2H) was attributed to the methylene introduced by piperazine in Abe, δ1.4−1.6 (m, 3H) was the methyl peak introduced by Flu, and δ4.41 (m, 1H) was attributed to the proton of the isopropyl of Flu (Figure 1A). In the infrared spectrum of AF, 1700 cm^{-1} (amide I band) could be attributed to the stretching vibration of C═O of Flu and disappearance of the stretching vibration of N−H of Abe at 3230 cm^{-1}, suggesting that the carboxyl group of Flu reacted with the secondary amine of Abe by amide bonding (Figure 1B). The time-of-flight (TOF)−MS showed that the m/z of $[M + H]^+$ of AF was 733.4502 and the m/z of $[M + 2H]^{2+}$ was 367.4577, which corresponded to the molecular weight of AF 732 (Figure 1C).

3.2. Stability Studies. Amide bonds had enough stability in buffers of pH 1.2 (0.2% SDS), pH 5.0 (0.2% SDS), and pH 6.8 (0.2% SDS) with degradation rates of 11.71, 7.77, and 4.55%, respectively, within 24 h. Enzyme catalysis was needed for the hydrolysis of amide bonds. Cathepsin B is a lysosomal protease, and lysosomal proteases are the most active at pH 5. Activated cathepsin B can accelerate the hydrolysis of amide bonds. As shown in Figure 1D, AF showed cathepsin B responsiveness in weak acid with degradation by 53.99% within 24 h at pH 5.0 (0.2% SDS) with the addition of cathepsin B. This property of AF increased the selectivity of drugs to the tumor microenvironment. AF also had good stability in artificial gastric fluid and artificial intestinal fluid (Figure 1E), which can reduce the distribution of Abe and NSAIDs in the gastrointestinal tract to protect the gastrointestinal tract from damage from free drugs. Such a finding might be caused by the large steric barrier of AF, which makes hydrolyzing amide bonds challenging. This was consistent with the results of the tissue distribution study.

3.3. Affinity of AF for CDK4/6. The molecular docking results are listed in Figure 2. The affinity scores of AF with 2w96 (CDK4 protein crystal) and 5L2T (CDK6 protein crystal) were −9.6 and −8.5 kcal/mol, respectively. In addition to interactions of PI-Cation, PI-Sigma, Pi-Alkyl, and AF had hydrogen bonding with SER B: 52, VAL B: 137, and CYS B: 135 in 2w96 and hydrogen bonding with TYR A: 292, ALA A: 291, and THR A: 198 in 5L2T, which was critical for ligand receptor affinity. It is evident from the molecular docking studies that AF, as a novel entity, had affinity for CDK4/6 enzymes to some extent. From the above results, AF not only exerts its potency through the release of original drugs *in vivo* but also has the ability to directly block tumor growth, which is associated with the results of pharmacodynamics and cytotoxicity.

3.4. Preparation and Characterization of Lys-PDA@AF NCs. As shown in Figure 3A, the XPS wide-scan spectra of AF showed F at 686 eV, and the electron flow intensity of F in the Lys-PDA@AF NCs decreased because the F in AF was shielded by PDA. The appearance of the C 1s spectrum at a binding energy of 288.1 eV on the surface of Lys-PDA@AF NCs was attributed to the presence of oxy-C═O in lysine. The content of O on the surface of Lys-PDA@AF NCs was 13.87%, higher than that on AF due to the presence of many hydroxyl and carboxyl groups in the structure of PDA and lysine, respectively (Figure 3B).[28] Meanwhile, in the FTIR spectrum of PDA, 1512 and 1580 cm^{-1} were the stretching vibrations of the C═C backbone in the aromatic ring of PDA, and 1700 cm^{-1} was the stretching vibration of C═C in the free lysine (Figure 3C). Overall, the XPS and FTIR results suggested that Lys-PDA was successfully coated onto the nanocrystals.

As shown in Figure 3D, AF released 70.7% in pH 1.2 (0.2% SDS) medium, within 2 h. In contrast, only 3.6% of AF was released from Lys-PDA@AF NCs within the same time period. The gastric emptying time was 2 h, which suggested that the released AF was able to remain stable until they reached the intestine. Meanwhile, 58.2% of Lys-PDA@AF NCs were released at pH 6.8 (0.2% SDS) within 48 h. Lys-PDA had an impact on the drug release behavior and could extend the residence time of the active substance *in vivo* (Figure 3E). The dense coating structure of PDA, which can prevent gastric acid erosion, may be the cause of this release behavior.

The average particle size of Lys-PDA@AF NCs was 224.9 ± 2.53 nm, and the polydispersity coefficient was 0.141 ± 0.014. The lysine shielded part of the negative charge of PDA, making the nanoparticles nearly electrically neutral with a zeta potential of −8.77 ± 1.5 mV. The size and potential were beneficial for improving intestinal penetration. Meanwhile, TEM images showed that the bare nanocrystals were spherical, and a thin film could be seen on the surface of the Lys-PDA@AF NCs (Figure 3F). The drug loading of Lys-PDA@AF NCs

https://doi.org/10.1021/acsomega.3c10142
ACS Omega 2024, 9, 18137−18147

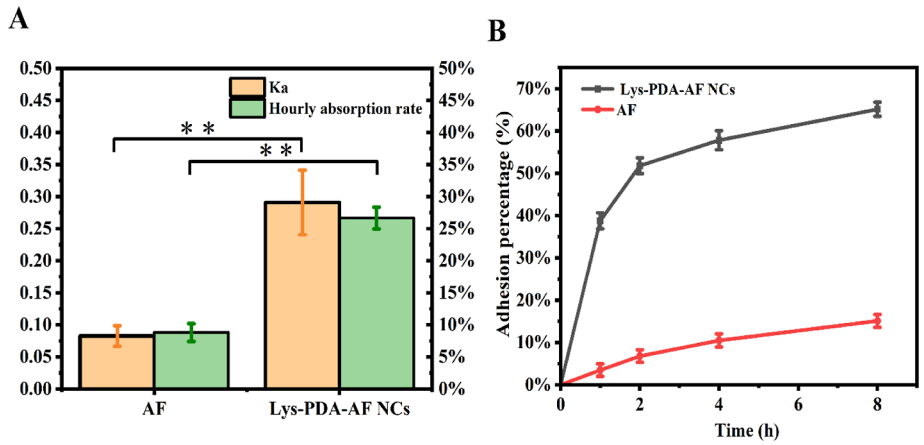

Figure 5. (A) Ka and hourly absorption rate of AF in different groups. (B) Adhesion percentage of AF in different groups. Data are exhibited as mean ± SD (n = 5).*P < 0.05, **P < 0.01, and ***P < 0.001.

was 32.6 ± 1.3%. This finding could be explained by the presence of numerous active groups in PDA.

3.5. *In Vitro* Cytotoxicity. The cytotoxicity and CI of the drugs were analyzed by the MTT method. Abe significantly inhibited cell viability by 52 and 56% (at concentrations of 40 and 80 μg/mL, respectively), and Flu alone had almost no cytotoxicity (Table S7). However, the cell viability inhibition rate was significantly increased when Abe and Flu were used together in cotherapy. The Lys-PDA@AF NCs showed a cell viability inhibition rate of 68% at 80 μg/mL (Figure 4A). The IC_{50} values of Abe, the physical mixture (Abe + Flu), and Lys-PDA@AF NCs were 22.03, 7.75, and 4.86 μg/mL, respectively (Figure 4B). Lys-PDA@AF NCs had favorable cytotoxicity because they have affinity for CDK4/6 enzymes. Moreover, Abe and Flu were synergistic (the CI was 0.35).

3.6. Evaluation of Intestinal Absorption of Lys-PDA@AF NCs. The whole segment from the duodenum to the ileum was used as the study subject. Phenol red is not absorbed by the small intestine and was used to determine the amount of absorbed water. The results showed that the absorption rate constant (Ka) of the rare codrug was 0.064/h, while the absorption rate constant of Lys-PDA@AF NCs was increased by 5 times (Figure 5A). Meanwhile, the hourly absorption rate increased from 7.2 to 28.8%. The modification of lysine made the nanoparticles nearly electrically neutral, which led to an increase in intestinal permeability. Because mucus is positively charged, electrically neutral particles have no charge interaction with mucus and therefore have better mucus penetration.[22]

Moreover, the mucus adhesion of PDA was evaluated using a mucin-binding assay. The binding rate of Lys-PDA@AF NCs to mucin reached 65.1% at 8 h (Figure 5B). In contrast, the binding rate of AF to mucin was 15.1% within the same period. This difference was explained by the chemical similarity between PDA and the mussel adhesion protein as well as the fact that amino and hydroxyl groups enriched on the surface of PDA increased adhesion to the intestine through noncovalent interactions.

In addition, the large specific surface area of nanoparticles, which is easily captured by mucus, can increase the passive diffusion of drugs to achieve transcellular transport. Lys-PDA@AF NCs have a suitable particle size, which increases the level of endocytosis of nanoparticles by the cell membrane. These are also the reasons Lys-PDA@AF NCs can improve the drug intestinal absorption.

3.7. Pharmacokinetics and Tissue Distribution Study. The concentration−time curves of Abe, Flu, and AF in the physical mixture (Abe + Flu) and Lys-PDA@AF NC groups are shown in Figure 6 (A/B/C). The main pharmacokinetic parameters for each group are listed in Tables S4−S6. When compared to those of the physical mixture (Abe + Flu) group, the $t_{1/2}$ and AUC values of Flu in Lys-PDA@AF NCs were approximately 3.6 and 2.5 times higher, respectively. Meanwhile, the $t_{1/2}$ and AUC of Abe in the Lys-PDA@AF NC group were much higher than those in the physical mixture (Abe + Flu) group (5.1 and 2.5 times, respectively). Such findings could be attributed to the Lys-PDA@AF NCs yielding a better oral absorption to increase the AUC, and it will take some time for AF to be released from Lys-PDA. More importantly, the $t_{1/2}$ and t_{max} of Abe and Flu differed greatly in the physical mixture (Abe + Flu) group, whereas both original drugs in the Lys-PDA@AF NC group reached peak concentrations almost simultaneously with similar t_{max}, which could improve the efficacy and safety.

The comparison of drug concentrations in tissues of the physical mixture (Abe + Flu) and Lys-PDA@AF NC groups is shown in Figure 6D−G. The concentrations of Flu and Abe in the stomach were much lower in the Lys-PDA@AF NC groups than in the physical mixture (Abe + Flu) group because PDA can be stable in the stomach. Reduction of gastric and cardiac levels of Flu may reduce the gastric and cardiac toxicity of NSAIDs. The fact that PDA is extremely sticky to promote oral absorption is the reason for the elevated levels of both original drugs in the Lys-PDA@AF NC group. In addition, the peak concentrations in all tissues of the Lys-PDA@AF NC group were lower than those of the physical mixture (Abe + Flu) group, which may reduce toxicity to normal tissues.

3.8. *In Vivo* Antitumor Activity. Figure 7B,C demonstrated that the CT26 tumor growth rate in the control group was higher than that in the other groups after the tumor model was formed in Bal B/C mice. In addition, the Lys-PDA@AF NC groups (inhibition rate was 52.49%) showed stronger antitumor activity than the physical mixture (Abe + Flu) group (inhibition rate was 29.7%) (Figure 7C). Lys-PDA@AF NCs showed the best antitumor effect, which could be attributed to the increased intestinal absorption and better cytotoxicity of

https://doi.org/10.1021/acsomega.3c10142
ACS Omega 2024, 9, 18137−18147

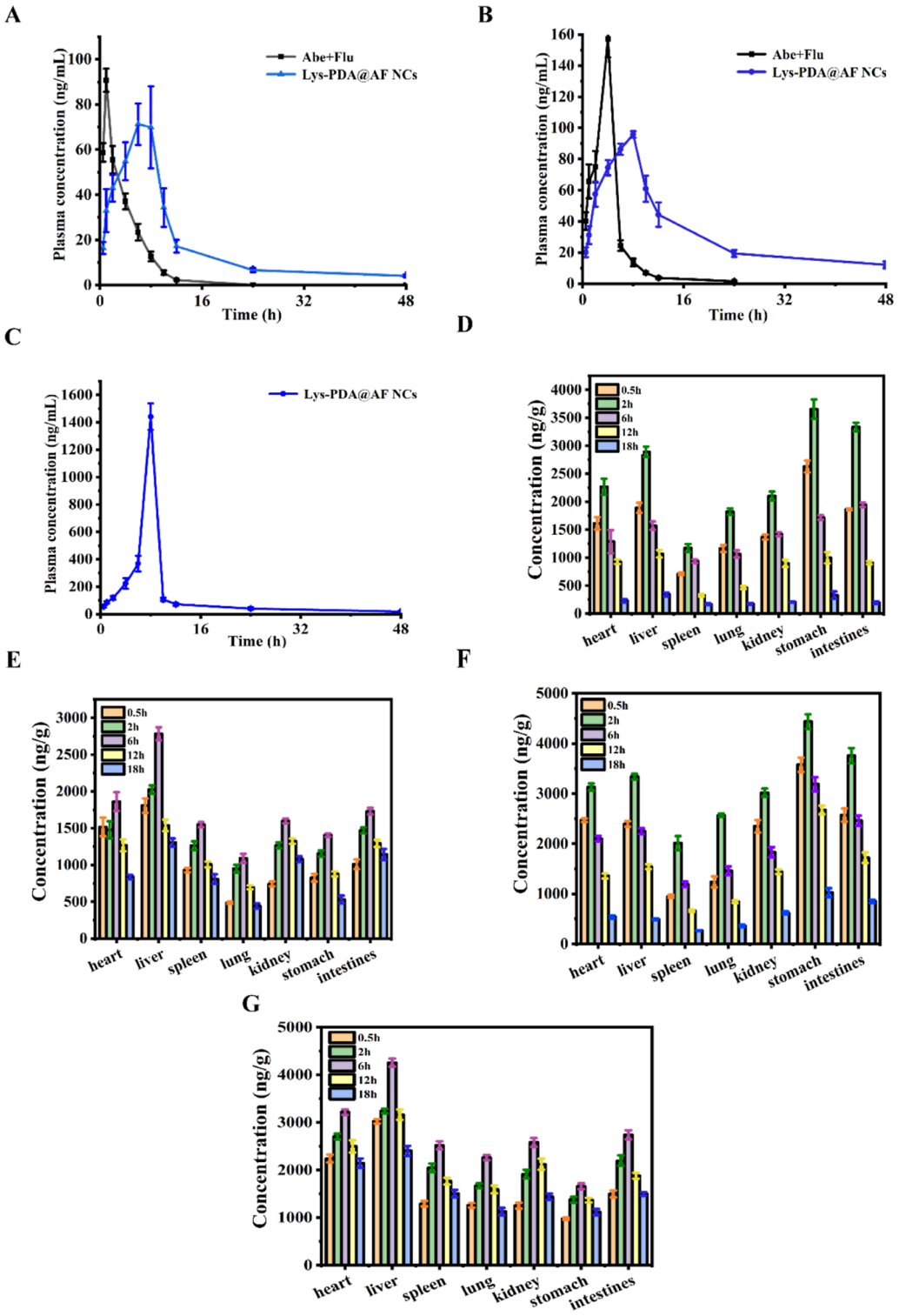

Figure 6. (A) Concentration−time curves of Flu. (B) Concentration−time curves of Abe. (C) Concentration−time curves of AF. (D) Concentrations of Flu in tissues in the physical mixture (Abe + Flu) group. (E) Concentrations of Flu in tissues in the Lys-PDA@AF NC group. (F) Concentrations of Abe in tissues in physical mixture (Abe + Flu) group. (G) Concentrations of Abe in tissues in Lys-PDA@AF NC group. n = 6.

AF. The aforementioned findings agreed with those made *in vitro*.

Meanwhile, TNF-α and IL-6 in tumor tissues were measured by the ELISA method. Lys-PDA@AF NCs were able to lower the inflammatory factors TNF-α and IL-6 to almost normal levels, which were attributed to the Flu produced by AF. By inhibiting inflammatory factors and regulating the tumor microenvironment, Flu was able to enhance the antitumor activity of Abe (Figure 7D).

Moreover, from the TUNEL and HE staining of tumor tissue sections, it could be observed that the physical mixture (Abe + Flu) group had a certain degree of necrosis and

https://doi.org/10.1021/acsomega.3c10142
ACS Omega 2024, 9, 18137−18147

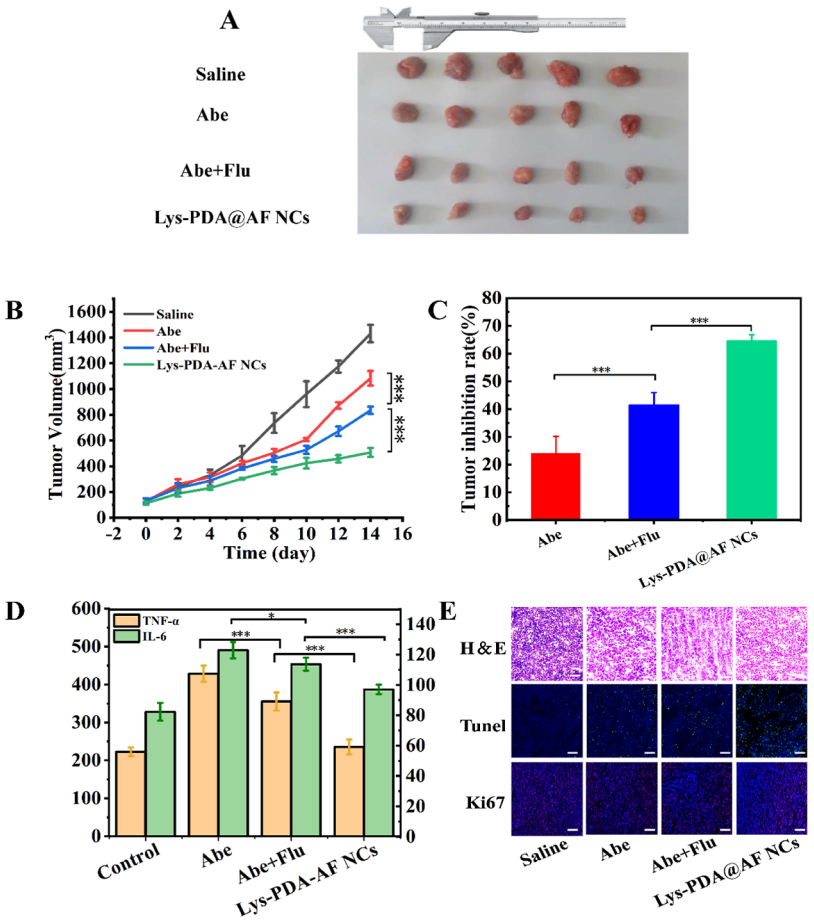

Figure 7. Pharmacodynamics. (A) Images of tumor size after treatment with different drugs. (B) Tumor volume growth curve. (C) Tumor inhibition rate. (D) TNF-α and IL-6 at the tumor site after treatment. (E) HE, TUNEL, and Ki67 staining of tumors at the end point of the assay (scale bar, 100 μm). Data are exhibited as mean ± SD (n = 5).*P < 0.05, **P < 0.01, and ***P < 0.001.

apoptosis, while the tumor cells in the Lys-PDA@AF NC group showed a large area of necrosis and apoptosis. The Ki67 results showed that Lys-PDA@AF NCs suppressed tumor angiogenesis and the growth of cancer cells (Figure 7E).

Above all, the findings of Lys-PDA@AF NCs with stronger antitumor activity may be attributed to the following reasons: Lys-PDA increased intestinal absorption of codrug, thereby increasing the bioavailability of both codrug and its parent drugs. Moreover, because of the overexpression of cathepsin B in tumor tissue, most AF was hydrolyzed as original drugs at the tumor site to exert its efficacy. In addition, as a new entity, AF itself also had antitumor activity, which can be concluded from the results of macromolecular docking and cytotoxicity.

3.9. Safety Evaluation. Chemotherapeutic drugs can cause serious systemic toxic effects due to their nonspecific distribution. In our study, no significant reductions in leukocytes, platelets, or neutrophils were observed in the Lys-PDA@AF NC groups. Meanwhile, liver and kidney function indices (AST, ALT, BUN, and CR) were normal (Figure 8B–D). As shown in Figure 8A, HE sections of major tissues (heart, liver, spleen, lung, and kidney) also did not show significant damage. This result indicated that the Lys-PDA@AF NCs had relative safety.

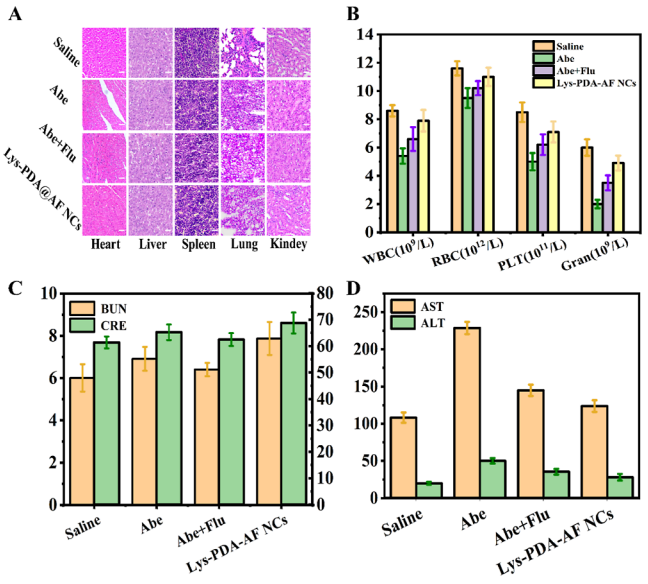

Figure 8. Toxicities and intestinal absorption. (A) HE staining of heart, liver, spleen, lung, and kidney (scale bar,100 μm). (B) WBC, RBC, PLT, and Gran of mice. (C) Hepatotoxicity of mice. (D) Nephrotoxicity of mice.

4. CONCLUSIONS

In this study, Lys-PDA@AF NCs were developed, which achieved the expected improvements in efficacy, safety, and oral absorption for combination therapy. The results suggested that the codrug gave the original drugs identical pharmacoki-

https://doi.org/10.1021/acsomega.3c10142
ACS Omega 2024, 9, 18137−18147

netic properties, which increased the safety and synergistic effect of Abe and Flu. Meanwhile, Lys-PDA@AF NCs reduced the distribution of the original drugs in the stomach, which decreased the gastrointestinal toxicity of oral administration. Additionally, oral absorption was improved by PDA modified with lysine, which increased the anticancer effectiveness. Compared to the physical mixture (Abe + Flu), Lys-PDA@AF NCs prolonged the circulation time of each agent and increased the effect and safety. We believe that the preparation of codrugs into nanocrystals and encapsulation in PDA modified with lysine are effective strategies for combining NSAIDs with chemotherapeutic agents for the oral treatment of tumors.

■ ASSOCIATED CONTENT

Supporting Information

The Supporting Information is available free of charge at https://pubs.acs.org/doi/10.1021/acsomega.3c10142.

Chromatographic conditions for different experiments, mass spectrometric conditions for pharmacokinetic study, and pharmacokinetic parameters (PDF)

■ AUTHOR INFORMATION

Corresponding Authors

Ji Li − *Department of Pharmaceutics, School of Pharmacy, Shenyang Pharmaceutical University, Shenyang 110016, PR China*; Email: syphuliji@163.com

Dongkai Wang − *Department of Pharmaceutics, School of Pharmacy, Shenyang Pharmaceutical University, Shenyang 110016, PR China*; orcid.org/0000-0002-4081-8443; Email: wangycsyphu@126.com

Zhiguo Yu − *Department of Pharmaceutics, School of Pharmacy, Shenyang Pharmaceutical University, Shenyang 110016, PR China*; orcid.org/0000-0003-1493-8932; Email: zhiguo-yu@163.com

Authors

Ting Sun − *Department of Pharmaceutics, School of Pharmacy, Shenyang Pharmaceutical University, Shenyang 110016, PR China*

Faxing Zhang − *Department of Pharmaceutics, School of Pharmacy, Shenyang Pharmaceutical University, Shenyang 110016, PR China*

Yuyi Xu − *Department of Pharmaceutics, School of Pharmacy, Shenyang Pharmaceutical University, Shenyang 110016, PR China*

Xiaowei Wang − *Nanjing University Medical School Affiliated Nanjing Drum Tower Hospital, Nanjing 210000, PR China*

Jiajia Jia − *Department of Pharmaceutics, School of Pharmacy, Shenyang Pharmaceutical University, Shenyang 110016, PR China*

Lihong Sang − *Department of Pharmacy, Gansu Wuwei Tumor Hospital, Wuwei 733000, PR China*

Complete contact information is available at: https://pubs.acs.org/10.1021/acsomega.3c10142

Author Contributions

Ting Sun: conceptualization, writing—original draft, data curation, writing—review and editing, and visualization. **Faxing Zhang**: investigation and validation. **Yuyi Xu and Xiaowei Wang**: software. **Jiajia Jia and Lihong Sang**: methodology and formal analysis. Ji Li: supervision. **Dongkai Wang**: project administration and funding acquisition. **Zhiguo Yu**: project administration and resources.

Notes

The authors declare no competing financial interest.

All animal experimental protocols were approved by Shenyang Pharmaceutical University, and the animal experiments met the requirements of the Ethical Guidelines for Investigations in Laboratory.

■ ACKNOWLEDGMENTS

Characterization measurements were performed at Kwak Xia Pharmaceutical Technology (Liaoning) Co., Ltd. Furthermore, the authors acknowledge the servicebio, for the Pharmacological research.

■ REFERENCES

(1) Bae, H. J.; Kang, S. K.; Kwon, W. S.; Jeong, I.; Park, S.; Kim, T. S.; Kim, K. H.; Kim, H.; Jeong, H. C.; Chung, H. C.; et al. P16 methylation is a potential predictive marker for abemaciclib sensitivity in gastric cancer. *Biochem. Pharmacol.* **2021**, *183*, 114320.

(2) Thoma, O. M.; Neurath, M. F.; Waldner, M. J. Cyclin-dependent kinase inhibitors and their therapeutic potential in colorectal cancer treatment. *Front. Pharmacol* **2021**, *12*, 757120.

(3) Ansarinik, Z.; Kiyani, H.; Yoosefian, M. Investigation of self-assembled poly (ethylene glycol)-poly (L-lactic acid) micelle as potential drug delivery system for poorly water soluble anticancer drug abemaciclib. *J. Mol. Liq.* **2022**, *365*, 120192.

(4) Pacal, I.; Karaboga, D.; Basturk, A.; Akay, B.; Nalbantoglu, U. A comprehensive review of deep learning in colon cancer. *Biol. Med.* **2020**, *126*, 104003.

(5) Cao, W.; Chen, H. D.; Yu, Y. W.; Li, N.; Chen, W. Q. Changing profiles of cancer burden worldwide and in China: a secondary analysis of the global cancer statistics 2020. *Chin. Med. J.* **2021**, *134* (7), 783−791.

(6) Schmitt, M.; Greten, F. R. The inflammatory pathogenesis of colorectal cancer. *Nat. Rev. Immunol.* **2021**, *21*, 653−667.

(7) Fantini, M. C.; Guadagni, I. From inflammation to colitis-associated colorectal cancer in inflammatory bowel disease: Pathogenesis and impact of current therapies. *Dig. Liver Dis.* **2021**, *53*, 558−565.

(8) Cai, Y.; Yousef, A.; Grandis, J. R.; Johnson, D. E. NSAID therapy for PIK3CA-Altered colorectal, breast, and head and neck cancer. *Adv. Biol. Regul.* **2020**, *75*, 100653.

(9) Regulski, M.; Regulska, K.; Prukała, W.; Piotrowska, H.; Stanisz, B.; Murias, M. COX-2 inhibitors: a novel strategy in the management of breast cancer. *Drug Discovery Today* **2016**, *21* (4), 598−615.

(10) Song, X. Q.; Ma, Z. Y.; Wu, Y. G.; Dai, M. L.; Wang, D. B.; Xu, J. Y.; Liu, Y. New NSAID-Pt(IV) prodrugs to suppress metastasis and invasion of tumor cells and enhance anti-tumor effect in vitro and in vivo. *Eur. J. Med. Chem.* **2019**, *167*, 377−387.

(11) Alqahtani, M. S.; Kazi, M.; Alsenaidy, M. A.; Ahmad, M. Z. Advances in Oral Drug Delivery. *Front. Pharmacol* **2021**, *12*, 618411.

(12) Xu, Y.; Shrestha, N.; Préat, V.; Beloqui, A. Overcoming the intestinal barrier: A look into targeting approaches for improved oral drug delivery systems. *J. Controlled Release* **2020**, *322*, 486−508.

(13) Modi, N. D.; Abuhelwa, A. Y.; Badaoui, S.; Shaw, E.; Shankaran, K.; McKinnon, R. A.; Rowland, A.; Sorich, M. J.; Hopkins, A. M. Prediction of severe neutropenia and diarrhoea in breast cancer patients treated with abemaciclib. *Breast* **2021**, *58*, 57−62.

(14) El-Shahawy, A.; Zohery, M.; El-Dek, S.; El-Dek, S. I. Theranostics platform of Abemaciclib using magnetite @silica@chitosan nanocomposite. *Int. J. Biol. Macromol.* **2022**, *221*, 634−643.

(15) Maniewska, J.; Jeżewska, D. Non-steroidal anti-inflammatory drugs in colorectal cancer chemoprevention. *Cancers* **2021**, *13*, 594.

(16) Rolim, M. de O. P.; de Almeida, A. R.; da Rocha Pitta, M. G.; de Melo Rêgo, M. J. B.; Quintans-Júnior, L. J.; Quintans, J. de S. S.;

Heimfarth, L.; Scotti, L.; Scotti, M. T.; da Cruz, R. M. D.; et al. Design, synthesis and pharmacological evaluation of CVIB, a codrug of carvacrol and ibuprofen as a novel anti-inflammatory agent. *Int. Immunopharmacol.* **2019**, *76*, 105856.
(17) Sloane, B. F.; Yan, S.; Podgorski, I.; Linebaugh, B.; Cher, M.; Mai, J.; Cavallomedved, D.; Sameni, M.; Dosescu, J.; Moin, K. Cathepsin B and tumor proteolysis: contribution of the tumor microenvironment. *Semin. Cancer Biol.* **2005**, *15*, 149−157.
(18) Wang, Y.; Wang, X.; Deng, F.; Zheng, N.; Liang, Y.; Zhang, H.; He, B.; Dai, W.; Wang, X.; Zhang, Q. The effect of linkers on the self-assembling and anti-tumor efficacy of disulfide-linked doxorubicin drug-drug conjugate nanoparticles. *J. Controlled Release* **2018**, *279*, 136−146.
(19) Guo, K.; Ma, X.; Li, J.; Zhang, C.; Wu, L. Recent advances in combretastatin A-4 codrugs for cancer therapy. *Eur. J. Med. Chem.* **2022**, *241*, 114660.
(20) Markovsky, E.; Baabur-Cohen, H.; Satchi-Fainaro, R. Anticancer polymeric nanomedicine bearing synergistic drug combination is superior to a mixture of individually-conjugated drugs. *J. Controlled Release* **2014**, *187*, 145−157.
(21) Tian, Z.; Mai, Y.; Meng, T.; Ma, S.; Gou, G.; Yang, J. Nanocrystals for Improving Oral Bioavailability of Drugs: Intestinal Transport Mechanisms and Influencing Factors. *AAPS PharmSciTech* **2021**, *22*, 179.
(22) Netsomboon, K.; Bernkop-Schnürch, A. Mucoadhesive vs. mucope-netrating particulate drug delivery. *Eur. J. Pharm. Biopharm.* **2016**, *98*, 76−89.
(23) Hu, S. S.; Yang, Z.; Wang, S.; Wang, L.; He, Q.; Tang, H.; Ji, P.; Chen, T. Zwitterionic polydopamine modified nanoparticles as an efficient nanoplatform to overcome both the mucus and epithelial barriers. *Chem. Eng. J.* **2022**, *428*, 132107.
(24) Jin, A.; Wang, Y.; Lin, K.; Jiang, L. Nanoparticles modified by polydopamine: Working as "drug" carriers. *Bioact. Mater.* **2020**, *5*, 522−541.
(25) Poinard, B.; Kamaluddin, S.; Tan, A. Q. Q.; Neoh, K. G.; Kah, J. C. Y. Polydopamine coating enhances mucopenetration and cell uptake of nanoparticles. *ACS Appl. Mater. Interfaces* **2019**, *11*, 4777−4789.
(26) Li, H.; Yin, D.; Li, W.; Tang, Q.; Zou, L.; Peng, Q. Polydopamine-based nanomaterials and their potentials in advanced drug delivery and therapy. *Colloids Surf., B* **2021**, *199*, 111502.
(27) Wang, X.; Zhao, H.; Liu, Z.; Wang, Y.; Lin, D.; Chen, L.; Dai, J.; Lin, K.; Shen, S. G. Polydopamine nanoparticles as dual-task platform for osteoarthritis therapy: A scavenger for reactive oxygen species and regulator for cellular powerhouses. *Chem. Eng. J.* **2021**, *417*, 129284.
(28) Kim, S. H.; In, I.; Park, S. Y. pH-Responsive NIR-Absorbing Fluorescent Polydopamine with Hyaluronic Acid for Dual Targeting and Synergistic Effects of Photothermal and Chemotherapy. *Biomacromolecules* **2017**, *18*, 1825−1835.

https://doi.org/10.1021/acsomega.3c10142
ACS Omega 2024, 9, 18137−18147